Universiteit Utrecht

Utrecht University

Institute for Theoretical Physics

Bachelor's thesis

Dynamics of charged particles dissolved in water in an electrolytic cell

Author:
Sander Kempkes
3473554

Supervisors:
Prof. Dr. René van Roij
Dr. Andreas Härtel
Mathijs Janssen, M.Sc.

Abstract

When fresh water and seawater meet, a huge amount of entropy is produced due to ionic mixing. This entropy leads to a dissipation of free energy at river mouths. At the moment, a lot of research is being done on this process to harvest this so-called (clean) *blue energy*. Multiple cycles have been proposed to generate the maximum energy per cycle and make use of the equilibrium potential and density profiles to calculate this energy. However, when the maximum amount of work or energy per time is being researched, the dynamics of the dissolved charged particles in water must be taken into account. This research focuses on these dynamics of charged particles in an electrolytic cell and aims to to describe the potential and density profiles for three different electrolytic cell models. We use the Poisson-Boltzmann equation and a set of numerical techniques to analyze these models. We first describe the Posson-Boltzman equation in the standard Gouy-Chapman-Stern model and extend this view to the Modified Poisson-Boltzmann equation. Thereafter, we develop a method to describe the dynamics in an electrolytic cell by combining the Poisson-Boltzmann equation and the Nernst-Planck equation.

January 15, 2014

Preface

In the last six months, my fellow student Sam Eigenhuis and I have been working on this so-called blue energy project within our BachelorONderZoek (BONZ). A very interesting and promising project in which I spend my hours happily. Especially working together with Sam, and the guidance from Mathijs, Andreas and René made this project a nice masterpiece of my bachelor.

Since a long time I have been interested in sustainable ways to generate energy. I think a sustainable way of living is crucial for the future of our planet. Energy is one of the most important and most scarce resources on the planet so if we can generate energy in a sustainable way, the world will be a better place for human kind. For this reason I started to study Science & Innovation Management in Utrecht wherein I wanted to discovered the world of photovoltaïcs, nuclear plants and wind turbines, and learn how these methods could be implemented in real-life. However, the physics in this bachelor was not detailed enough for me to learn about engines, energy and how we can create energy in a sustainable way. I was specifically frustrated when I took a course in Physical Chemistry wherein terms like entropy, Gibbs free energy and enthalpy were only briefly discussed. Entropy, as the teacher of this course, Andrew Bale, described it, can be explained in two ways. To start with, it can be described as (1) the amount of chaos in the only closed system we will ever know: the universe. Or it can be seen (2) when I leave my child in his bedroom and come back after five minutes. I was intrigued by this new concept of entropy, which was totally different from energy, made time 'flow' and decided the outcome of chemical reactions. I needed to broaden my research on sustainable energy and entropy by studying the laws of physics in the bachelor Physics and Astronomy in Utrecht.

In the second year of Physics and Astronomy I took the obligatory course Statistical Physics 1. Our professor for the first part of the course, René van Roij has been an enthusiastic teacher and introduced us to the concepts I was looking for: entropy and (free) energy. When René talked about his own works on blue energy, I was fascinated by the pictures of the engines he showed us. Moreover I was shocked by the large amount of free energy that is dissipated at river mouths. I knew what kind of topic I wanted to research during my BONZ, and contacted René about this project. At the begin of September, Sam and I started our BONZ.

Luckily Mathijs and Andreas, who were in team Blue Energy together with René, were very helpful and wanted to guide us during this project. At the start of this project, Sam and I barely knew what a blue engine is and how energy could be extracted from ionic movement in porous electrolytes that have a width of only 2 nm. We worked our way trough literature by Boon and Kornyshev, talked about the Brogioli cycle and began to understand more and more about the blue engine. We learned how to work with C++ of Microsoft Visual, made our first pictures with Gnuplot and explored various numerical methods, in which the shooting method and tridiagonal matrix method are the most important. After ten weeks, we were able to describe the ionic movement in equilibrium and we replicated data that Boon and Kornyshev found in their works. Because the BONZ is an individual project, Sam's and my path separated in the last ten weeks. Sam investigated the temperature gradient more intensively and wanted to calculate the optimal temperature of salt and fresh water to gain the maximal power output of the blue engine. My task was to investigate how the ions in the blue engine diffuse in time and what the potential profiles look like. Moreover, it is also interesting to increase the charges on the plate slowly and to see how the system responds.

And now the project is completed. In front of you lies the report I made after a half year's work and research. Sam and I spend many hours in the dark Minnaert computer room, discussed our problems every Monday at 10.00 with Mathijs and Andreas and discovered the science of Condensed-Matter during the weekly talks. I think most bachelor students do not like the BONZ because of the broad topic, the hard work and the vagueness of the project. However this project has been very accurate, well defined and because of the hard work I think that Sam and I made a report we can be proud of. I want to thank Mathijs, Andreas and René for their extensive guidance and time they spent on this project. Mostly because of your knowledge, patience and enthusiasm, we have worked happily on this project and are now able to hand in our final reports. This project is water under the bridge now, but it may be that in the future we are charged up again and will continue working on this interesting topic of blue engines.

Contents

1 Introduction

It is commonly known that entropy is produced when two or more species mix. This is also the case when two species of the same kind, containing certain different thermodynamic properties, mix. The most intuitive example is a system containing hot and cold water: when mixing cold water and hot water, the water will finally get to an intermediary temperature. This new system has a higher entropy than the initial system of the hot water and cold water together. This view can be extended to other systems like the mixing of seawater and fresh water. The chemical potential of seawater and fresh water are different since the ion concentration of seawater is higher than fresh water. When seawater and fresh river water meet at river mouths, these two fluids mix irreversibly and thus produce a large amount of entropy. This production of entropy results in a dissipation of free energy about 2 kJ per liter of river water, which is equal to a waterfall of 200 m [1]. If this energy can be harvested, it is possible to generate clean energy that may produce 20% of the world's energy demand [2]. Therefore harvesting this so-called blue energy is an interesting challenge which has a lot of potential to be used in the future.

Blue energy can be harvested with a so-called blue engine like the one proposed by Ref. [3]. This blue engine consists of two charged porous electrodes, a couple of microns apart, that are in contact with water of varying salinity. The charged electrodes attract oppositely charged ions from the salt water. The ions diffuse into the pores of the electrode and screen the charges within the pores. Then fresh water is flushed through the electrodes and when the electrodes discharge, the ions diffuse back into the fresh water. Finally the fresh water is replaced by seawater again and the cycle restarts. In this way, the salt seawater becomes more fresh and the fresh water becomes more salt, which implies that mixing has been taken place. The entropy of mixing is converted into blue energy when the ions diffuse back and forward within different potential profiles between the electrodes.

A blue engine can only be devised with proper understanding from the behavior of ions in liquids, in which the Gouy-Chapman (GC) model and the Gouy-Chapman-Stern (GCS) model are the most basic models. The GC and GCS model describe ions as point-like particles and are the result of the combination of the Poisson equation and the mean field Boltzmann distribution to calculate the ionic densities and potential in an electrolyte. The combination of these equations is called the Poisson-Boltzmann equation. The GC and GCS models are good approximations when the surface charges on the electrodes is low [4]. However, in a blue engine the surface charge is quite high and therefore the models fail to explain this behavior correctly. Recently Ref. [5] rediscovered an analytical solution for a so-called Modified Poisson-Boltzmann (MPB) model that includes finite ion sizes. Although the MPB model cannot calculate all properties of the system analytically, this method resulted in a more physically appropriate solution for larger surface charges for the properties that can be calculated. However, these models describe the electrostatics in an electrolyte and assume an instantaneous equilibrium of the density and potential profiles. But when developing an engine, power optimization is one of the greatest challenges. Power is energy per time and therefore insight is required in the development of the system towards an equilibrium when electrodes are being charged. Modeling an instantaneous charge on the electrode is possible because $v_{electron} \approx c/10$, which is so quick that the response of charging the electrodes can be neglected. Modeling the ions imposes problems. Ions typically move with $< x^2 >= 2Dt$ (Brownian motion), where D, the diffusivity, is of the order 10^{-5} cm$^2/s$. This implies that the response of the ions in time can not be neglected and we can conclude that an instantaneous density profile does not describe the blue engine correct. This bachelor thesis aims to describe the motion of ions in time in an electrolytic cell in order to understand the dynamics of the blue engine better. Ref. [6] already described the ionic flow for a system of two oppositely charged electrodes separated by 61 nm, but the pore size for the used blue engine is only a couple of nanometers which results in different physics. For the development of the blue engine as proposed by Ref. [4], we aim to describe how ions flow within the pores of the electrodes in a 2 nm system. The Nernst-Planck equation for the diffusion of particles is used in combination with the Poisson-Boltzmann equation to describe the instantaneous time evolution of this system. Furthermore we will investigate how the ionic movement depends on the charging of the plates. This report investigates the amount of time that is needed for the system to relax in multiple situations.

First we start with describing the GC, the GCS and the MPB models and replicate the findings from Ref. [6]. Thereafter, we will model the porous electrodes of the blue engine like Ref. [4] and describe the potential and density profiles in time.

2 The Gouy-Chapman and the Gouy-Chapman-Stern model

The Gouy-Chapman (GC) model is one of the most basic models for an electrolyte in contact with a charged object. It was developed about a hundred years ago independently by Louis Georges Gouy [7] and David Chapman [8]. A simple GC model consists of one charged plate in contact with dissolved ions in water. The water of volume V contains a total number of point-like N_+ cations and N_- anions leading to a density $\rho_\pm = \frac{N_\pm}{V}$. The total charge distribution in this system is denoted as $Q(\vec{r})$ and includes both the charges of the ions and the charge on the electrodes. We assume that the ions can screen the charge on the electrode completely $Q(z)/e \leq N_+ + N_-$. If we now write down the Coulomb interaction between the ions and the charged electrode as $\psi(\vec{r}) = \int \frac{Q(\vec{r}')}{4\pi\epsilon_0\epsilon|\vec{r}-\vec{r}'|} d\vec{r}$ (SI-units), we can derive the Poisson equation as $\nabla^2\psi(\vec{r}) = -Q(\vec{r})/(\epsilon_0\epsilon)$. In these equations, ψ is the potential and ϵ (and ϵ_0) the dielectric constant (in vacuum). The density profiles $\rho_\pm(\vec{r})$ in the GC model are approximated by a mean-field Boltzmann distribution. If we now only focus on the z direction, the Boltzmann distribution yields $\rho_\pm(z) = \rho_s e^{\mp\beta e\psi(z)}$, where ρ_s is the bulk concentration for the assumption $\psi(z \to \infty) = 0$, e is the elementary charge and $\beta^{-1} = k_\mathrm{B}T$ with k_B the Boltzmann constant and T the temperature. The expression $\psi(z \to \infty) = 0$ is chosen to be zero, because the potential is required to vanish at an infinite distance of the electrode. The only charges in this system are the charge on the plate, denoted by σ, and the charged cations and anions in the liquid. Thus $Q = e(\rho_+(z) - \rho_-(z)) + \sigma\delta(z))$, where $\delta(z)$ is the Dirac delta function and gives a peak at $z = 0$. It is now convenient to introduce the dimensionless potential $\phi(z) = \frac{e\psi(z)}{k_\mathrm{B}T}$. Furthermore, we can write the boundary conditions (BCs) (i) $\phi(z \to \infty) = 0$ and (ii) if we integrate over the delta-function $\sigma\delta(z)$ at the electrode $\phi'(z) = \int_{0^-}^{0^+} \phi''(z)dz = -4\pi\lambda_\mathrm{B}\sigma$ with $\lambda_\mathrm{B} = \frac{e^2}{4\pi\epsilon_0\epsilon k_\mathrm{B}T}$ the Bjerrum length. Then, the previously mentioned Poisson equation and the Boltzmann equation are combined into the familiar Poisson-Boltzmann (PB) equation

$$\begin{aligned} \phi''(z>0) &= \frac{-4\pi e^2}{4\pi\epsilon_0\epsilon k_\mathrm{B}T}(\rho_+(z) - \rho_-(z)) = -4\pi\lambda_\mathrm{B}\rho_s(e^{-\phi(z)} - e^{\phi(z)}) = \kappa^2 \sinh(\phi(z)), && (1)\\ \phi(z \to \infty) &= 0, && (2)\\ \phi'(z=0) &= -4\pi\lambda_\mathrm{B}\sigma, && (3) \end{aligned}$$

in which we use the Debye length $\kappa^{-1} = \sqrt{8\pi\lambda_\mathrm{B}\rho_s}^{-1}$.

Even though this is a simplified model, the GC model provides useful information. One outcome is the analytic expression for the surface charge σ on the electrode in terms of the surface potential $\psi(0)$

$$\sigma_{GC} = \frac{\kappa}{2\pi\lambda_\mathrm{B}} \sinh\left(\frac{e\psi_{GC}(0)}{2k_\mathrm{B}T}\right). \quad (4)$$

Another outcome is the ionic double layer: counterions are attracted to the charged plate and are adsorbed on the plate due to electrostatic interactions. These counterions form a layer around the plate which in combination with the charged electrode form a so-called double layer. The double layer screens the charge on the plate completely and has a typical thickness of κ^{-1}. In reality, coions are attracted on their turn to the plate due to the Coulomb interactions and form a diffuse layer together with the counterions (see Fig: 1). This means that the GC model describes qualitatively how such a electrolytic cell works, but fails to describe the behavior quantitatively. Especially in areas close to the plate ($z < \kappa^{-1}$) or when the surface charge σ is large [4] the GC model is not well applicable. Therefore Stern suggested to combine the Helmholtz model (for $\kappa^{-1} < z$) and the GC model (for $\kappa^{-1} > z$) for small values of σ. In the Helmholtz model, an electrode treats the ions as another electrode and compensates for the fact that ions have a size in such a way the charges of the ions cannot be stuck to the electrode but rather have a small distance between the charges of the ion and the electrode [9]. The Helmholtz layer is often called a Stern layer.

The Gouy-Chapman-Stern (GCS) model is quantitatively valid for low surface charge σ and is often used to describe electric double layers. However, the surface potential of a blue engine is too high to be properly described with a GCS layer. One of the main problems is the point-like ions. In a real model, more ions are attracted to the plate when the surface charge σ increases. If particles are point-like particles, there is an *infinite* number of ions that can be adsorbed by the plate. In contrast, when the particles have a size and volume, there is a *finite* amount of particles that can be adsorbed in the first layer at the plate. Thus in order to describe a blue engine appropriately, the GCS model needs to be improved to describe particles with a finite size. The following section focuses on including a finite ion size in the model.

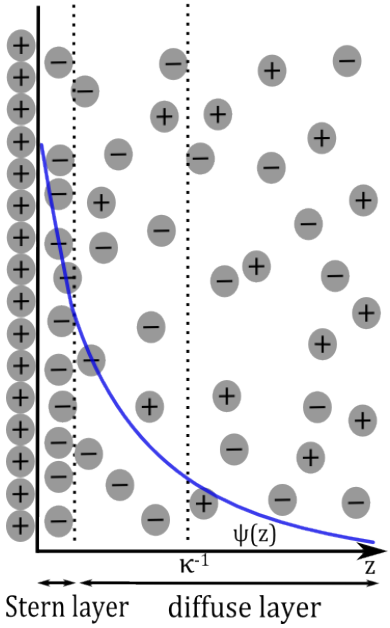

Figure 1: [2]Electric double layer in an electrolyte. Counterions are attracted to the electrode and form a Stern layer. Coins are attracted due to Coulomb interactions and form a diffuse layer together with counterions.

3 Modified Poisson-Boltzmann equation

Let us assume another, a more blue engine like model as described in Ref. [4]. We change our previous system to two oppositely charged electrodes width L apart instead of one electrode. Furthermore the ions now have a molecular volume v that needs to be taken into account. From Ref. [5] we know we can write the equilibrium density profiles as

$$\rho_{\pm}(z) = \frac{\rho_s e^{\mp\phi(z)}}{1-\eta_0+\eta_0\cosh(\phi(z))}, \tag{5}$$

where $\eta_0 = 2\rho_s v$ the ionic packing fraction of the reservoir. It is now easy to derive the PB-equation for this system:

$$\begin{aligned} \phi''(z) &= \frac{\kappa^2\sinh(\phi(z))}{1-\eta_0+\eta_0\cosh(\phi(z))}, & (6)\\ \phi'(z)|_{z=0} &= -4\pi\lambda_{\mathrm{B}}\sigma, & (7)\\ \phi'(z)|_{z=\frac{L}{2}} &= 0, & (8) \end{aligned}$$

with κ^{-1} again the Debye length. Eq. (6) with BCs (i) (7) and (ii) (8) cannot be solved analytically, but can be solved numerically. However, if we take $\kappa L \gg 1$ and $\eta_0 \ll 1$, we retrieve the GC expression Eq. (4) for the surface charge.

Another way to solve this Eq. (6) with BCs (i) (7) and (ii) (8) follows from Ref. [5]. When the PB-equation with respect to z is integrated and $\kappa L \gg 1$ the following equation can be derived

$$\frac{d\phi}{dz} = \mp\kappa\sqrt{\frac{2}{\eta_0}}\sqrt{\ln[1+2\eta_0\sinh^2(\frac{\phi(z)}{2})]}. \tag{9}$$

If we now make use of identity of Gauss law $-\epsilon\frac{d\psi}{dz} = 4\pi\sigma$, we can derive an equation which is quite similar to Eq. (4)

$$\sigma_{Kornyshev} = \frac{\kappa}{2\pi\lambda_{\mathrm{B}}\sqrt{2\eta_0}}\sqrt{\ln[1+2\eta_0\sinh^2(\frac{\phi(z)}{2})]}. \tag{10}$$

[2]Figure made by my fellow student Sam Eigenhuis

We can again approximate this expression with $\eta_0 \ll 1$, use $\ln[1+x] \approx x$ and regain Eq. (4). It is also possible to compare the GC and the MPB model in Fig. 2 where both curves are plotted. This was already done in Ref. [4], which uses the MPB equation to numerically calculate $\psi(0)$ as a function of σ. With the equations in Ref. [5], it is possible to redo these calculations analytically.

We observe in Fig. 2 that the analytical result from Ref. [5] agrees with the numerical result (figure 4) from

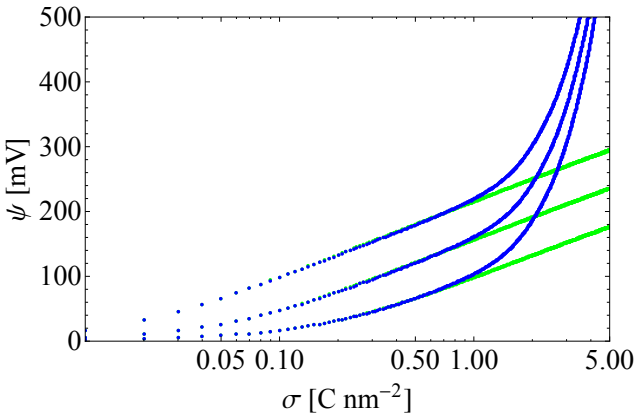

Figure 2: The surface potential of a planar electrode in contact with a half-space of electrolyte as a function of the surface charge density on the electrode. The green lines represents the GC limit from Eq. (4), while the blue line use the analytical expressions from Eq. (10). The salt concentrations of the reservoir vary from top to bottom as ρ_s ={1mM, 10mM, 100mM}.

Ref. [4]. The GC model breaks down beyond $\sigma = 0.5$ nm^{-2}, but can be used in combination with low surface charges.

As mentioned, the GC, GCS and MPB models all assume equilibrium density and potential profiles, but do not involve time or the diffusion of the ions. In order to investigate the dynamics in the blue engine, we need to incorporate the Nernst-Planck equation.

4 Dynamics in an electrolytic cell

The Nernst-Planck equation describes the motion of a chemical species in a fluid [6]. The equation can be derived from the continuity equation $\frac{\delta\rho_\pm}{\delta t} = -\nabla \cdot J_\pm$, wherein the flux of the ions $J_\pm$ is driven by density and potential gradients $J_\pm = \nabla\rho_\pm \pm \nabla\phi$. In this way, the Nernst-Planck equation extends Fick's law wherein only a concentration gradient is included in the equation. If we fill in the continuity equation with this $J_\pm$, we can write down the Nernst-Planck equation as

$$\frac{\delta\rho_\pm}{\delta t} = \nabla \cdot [D\nabla\rho_\pm \pm \frac{De}{k_\mathrm{B}T}\rho_\pm E], \tag{11}$$

where D is the diffusivity and $E = -\nabla\psi - \frac{\delta A}{\delta t}$ an electric field. The diffusivity can be calculated by using Einstein's relation $D = \frac{1}{6\pi\beta\eta a}$, in which again $\beta = (k_\mathrm{B}T)^{-1}$, η is the viscosity of the fluid and a the radius of a particle. The diffusivity is assumed to be constant in the blue engine and is assumed to be the same for the cations and the anions. In reality the diffusivity depends on the viscosity of fresh water (1.002 mPa s) and the viscosity of salt water (1.077 mPa s) [10], but the difference in D is negligible and therefore D can be taken as a constant. If we use the previous described model MPB containing two electrodes, we can rewrite Eq. (11) as

$$\begin{aligned}\frac{\partial\rho_\pm(t,z)}{\partial t} &= D\Big(\frac{\partial^2}{\partial z^2}\rho_\pm(t,z) \mp \frac{\partial}{\partial z}[\frac{e}{k_\mathrm{B}T}\rho_\pm(t,z)\frac{\partial}{\partial z}\psi(z,t)]\Big) \\ &= D\Big(\frac{\partial^2\rho_\pm(t,z)}{\partial z^2} \mp \frac{\partial}{\partial z}[\rho_\pm(t,z)\frac{\partial\phi(z,t)}{\partial z}]\Big)\end{aligned} \tag{12}$$

where $\phi(z,t) = \frac{e\psi(z,t)}{k_B T}$ is again the dimensionless potential. Eq. (12) can be used to numerically calculate the potential and density profiles at $t+\tau$. The process to calculate the potential and density profiles for every time step τ is as follows. At $t \leq 0$, the system is at rest with $\rho_{\pm,i} = \rho_s$. When at $t = 0$ an initial potential $\phi(-L/2)$ and $\phi(+L/2)$ are set respectively upon the left and right electrode we can write $\nabla^2\phi(t = 0, z) = 0$ because the ions did not have had any time to respond to the change of the charge on the electrodes. From this follows $\frac{\partial\phi(t=0,z)}{\partial z} = \frac{\Delta\phi}{L}$ and $\phi(t = 0, z) = \frac{\Delta\phi}{L}z$, where $\Delta\phi = \phi(L/2) - \phi(-L/2)$ is the difference between the potential on both electrodes. These equations can be filled in Eq. (12) and can be integrated to $t = \tau$ to determine the density profile $\rho_\pm(t = \tau, z)$ and $\frac{\partial^2\rho_\pm(t=\tau,z)}{\partial z^2}$. From the PB Eq. 1 $\frac{\partial^2\phi(t=\tau,z)}{\partial z^2} = -4\pi\lambda_B(\rho_+(t = \tau, z) - \rho_-(t = \tau, z))$ we can determine $\phi(t = \tau, z)$ and $\frac{\partial\phi(t=\tau,z)}{\partial z}$ as is explained in Sec. 7.1. These values are filled in into Eq. (12) to determine the density profiles at a later time. In Fig. 3, the used model at t =0 is given and the initial potential and density profiles are visible.

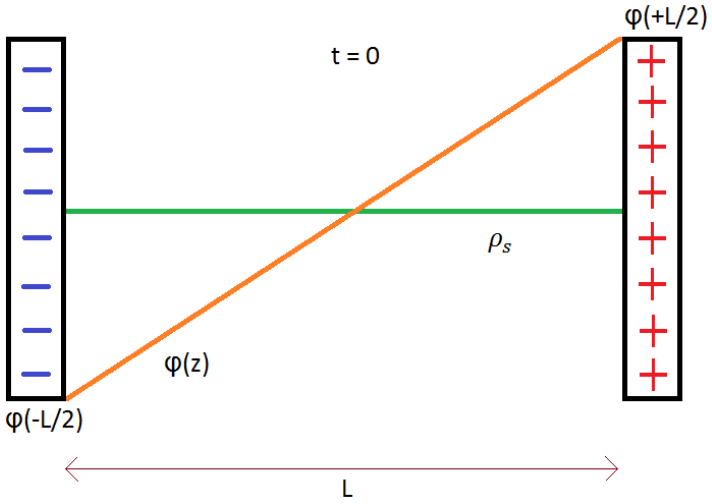

Figure 3: The used model in this research. The model describes two electrodes in contact with ions dissolved in water in planar geometry. The electrodes are oppositely charged at t =0, which results in $-\phi(-L/2, t = 0) = \phi(L/2, t = 0)$. The densities at t =0 are $\rho_\pm(z, t = 0) = \rho_s$.

With the Nernst-Planck equation we are able to calculate the movements of the ions and describe the dynamics in our model. We first apply the Nernst-Planck equation in combination with the PB-equation on the same model Ref. [6] uses and thereafter the equations are used upon a smaller model where the Debye lengths κ^{-1} are comparable with the width L of the model.

5 Numerical results

5.1 Replication Garlea

As mentioned, Ref. [6] already used a (different) method to determine how an electrolytic cell responds to an initial potential on the electrodes. Therefore, we can redo the calculations and verify the results. Ref. [6] uses a model consisting of two oppositely charged electrodes 61 nm apart. The ions have a size of 0.2 nm, which results in a diffusivity of $D = 1.1 * 10^{-9}$ m^2/s at a room temperature of 298 K. The ionic bulk concentration is $\rho_s = 10$mM, which results in a Debye length of $\kappa^{-1} = 0.289$ nm^{-1}. We introduce dimensionless quantities z^* and t^* just like Ref. [6] in order to perform the numerical calculations and compare the results. The spatial coordinate becomes $z^* = \kappa z$ and the time is expressed as $t^* = t\kappa^2 D = \frac{t}{\tau}$ where $\tau = \frac{1}{\kappa^2 D}$. In this way, τ can be seen as the time that an ion needs to diffuse over one Debye length. In this case, $\tau = 8.4$ ns. Furthermore we use the dimensionless potential $\phi(t, z) = \frac{e\psi(t,z)}{k_B T}$. In Fig. 4 and 5 the potential, density and flux profiles for a given $\phi(\pm L/2) = \pm 2$ on the electrodes are presented. Thereafter, the potential and density profiles for $\phi(\pm L/2) = \pm 4$ are given and an analysis is made on the equilibrium time. The figures represent the temporal

evolution of the system and reach the equilibrium values if $t \to \infty$. The figures are the same as in Ref. [6], which implies that the model and code work correctly.

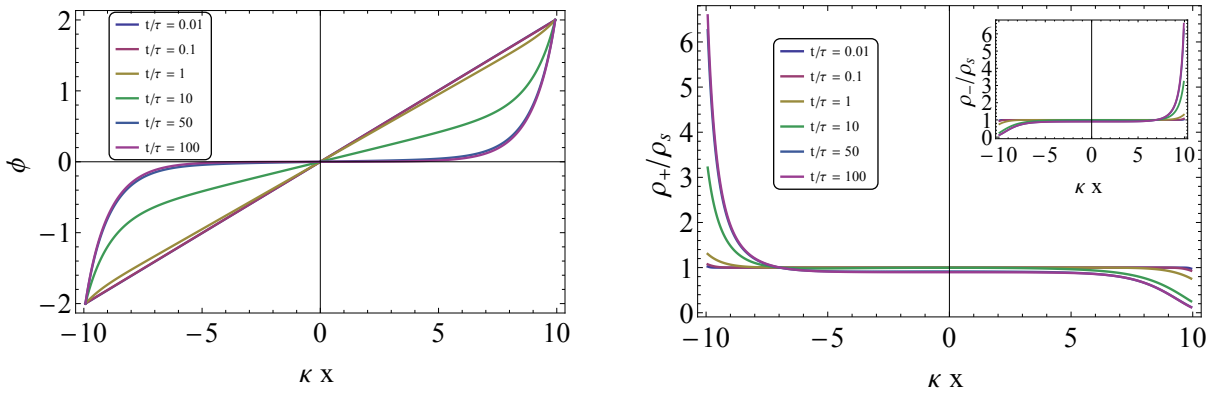

Figure 4: Potential and density profiles 61 nm system with opposite surface charges set at t=0 with $\phi(\pm L/2) = \pm 2$. The potential and density profiles shift in time from $t = 0.01\tau$ (blue) to $t = 0.1\tau$ (purple), $t = \tau$ (yellow), $t = 10\tau$ (green), $t = 50\tau$ (light blue) and $t = 100\tau$ (purple).

In these figures 4 we observe how the ions respond by setting an initial potential at $t = 0$ on the electrodes. At the start, the system responds slowly and after 1 diffusion time t/τ the system is almost in the same state as at $t = 0$. After $t/\tau = 10$ the ions moved quite a bit and after $t/\tau = 50$, the system has almost reached equilibrium. The cations are indeed attracted by the negative electrode at $-L/2$ and the anions are attracted by the positive electrode at $L/2$. Furthermore, we can distinguish the Debye length κ^{-1} where the potential and densities are influenced by the charged electrodes. After a couple of Debye lengths, the electrodes do not influence the system: the potential becomes approximately 0 and the density profiles are almost equal to ρ_s.

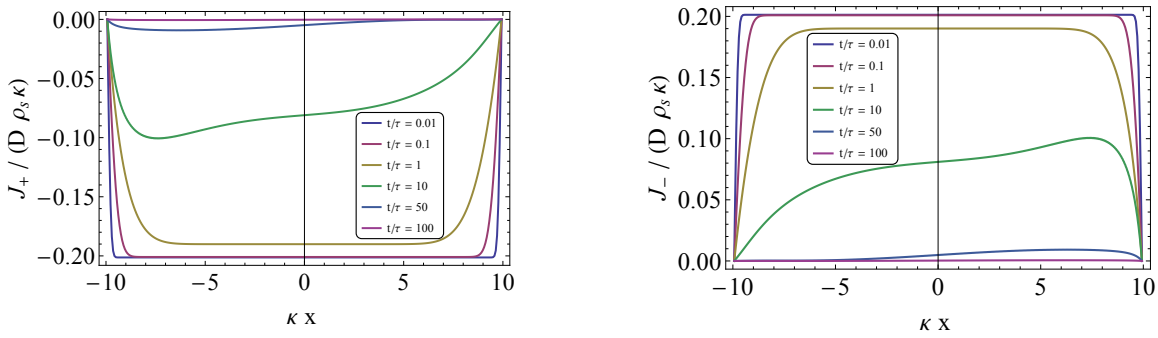

Figure 5: Rescaled (dimensionless) flux profiles 61 nm system with opposite surface charges set at t=0 with $\phi(\pm L/2) = \pm 2$. The flux profiles shift in time from $t = 0.01\tau$ (blue) to $t = 0.1\tau$ (purple), $t = \tau$ (yellow), $t = 10\tau$ (green), $t = 50\tau$ (light blue) and $t = 100\tau$ (purple). These figures are mirror images of each other.

The flux $J_\pm$ of the system is represented in Fig. 5. At the start, the flux of the ions is maximal and cations and anions are forced to flow towards the sides of the system. After $t/\tau = 1$, when only a small amount of charge on the electrodes has been screened, the flux decreases already and eventually becomes zero after $t/\tau = 100$. The asymmetry in the line t/τ=10 is due to the number of ions in that part of the model. For the J_+ figure, the largest number of ions is between $-L/2 < z \leq 0$ and therefore the gradient of the densities of the particles $\nabla\rho_+$ is higher in this region than in the other region of the model, and this results in an asymmetry of the flux.

If we now increase the potential on the electrodes $\phi(\pm L/2)$, the system needs more time to relax and reach equilibrium. In Fig. 6, this is shown when the potential is increased to $\phi(\pm L/2) = \pm 4$. At $t/\tau = 50$,

it is clear that the system needs more time than the $\phi(\pm L/2) = \pm 2$ system to reach equilibrium because the t/τ =50 and the t/τ =100 differ more in the $\phi(\pm L/2) = \pm 4$ case than in the $\phi(\pm L/2) = \pm 2$ case. Furthermore, we can see in Fig. 6 that the density profiles near the electrodes are higher than in the previous case because more ions are needed to screen the higher potential on the electrodes.

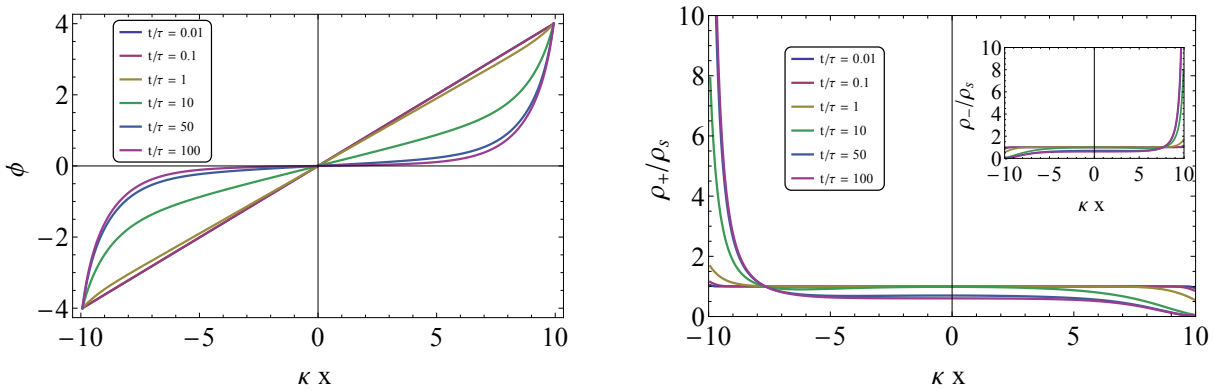

Figure 6: Potential and density profiles 61 nm system with opposite surface charges set at t=0. $\phi(\pm L/2) = \pm 4$. The potential and density profiles shift in time from $t = 0.01\tau$ (blue) to $t = 0.1\tau$ (purple), $t = \tau$ (yellow), t =10τ (green), t =50τ (light blue) and t =100τ (purple).

This notion can be analyzed further when looking at the densities for half the engine in Fig. 7 and for the surface charge $\sigma(\pm L/2)$ in Fig. 8.

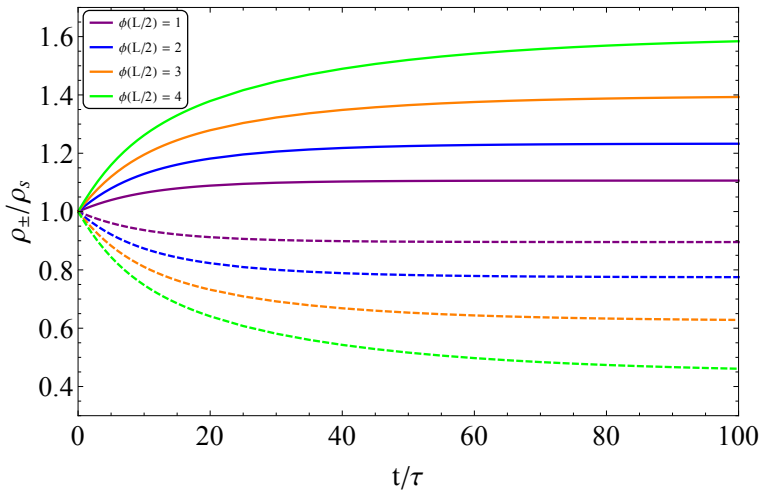

Figure 7: Addition of the ion densities for $-L/2 < z \leq 0$. The solid lines represent the addition of the densities of the cations and the dashed lines represent this addition for the anions. The time to reach equilibrium increases when the potential on the electrodes increases. Note that this system is symmetric and this figure can be mirrored in the z=0 plane to find the same profiles (only cations and anions switched around) for the right side of the model.

In Fig. 7, the densities for half of the model for different surface potential $\phi(\pm L/2)$ are added to determine how the ions move in the system. The figure shows three notably characteristics for each potential. Firstly, for a small potential, the system indeed needs less time to reach equilibrium. A small surface potential does not change this large system a lot and can be seen as a small perturbation. Therefore, the system will responds more quickly to a low surface potential than to a high surface potential. Secondly, more ions are

indeed needed to screen a larger potential. Thirdly, the number of ions is conserved in this model. When we add up the anions and cations at every point in the figure, we regain the value of $2\rho_s$. Because the system is symmetric, we can mirror the figure for the right side of the model and regain the same profiles for anions and cations (but now switched around). This implies number conservation in the model. The first notion about the equilibrium time can also be seen in for the surface charge in Fig. 8. We can use Eq.(3) to determine the surface charge on the electrodes at every time step.

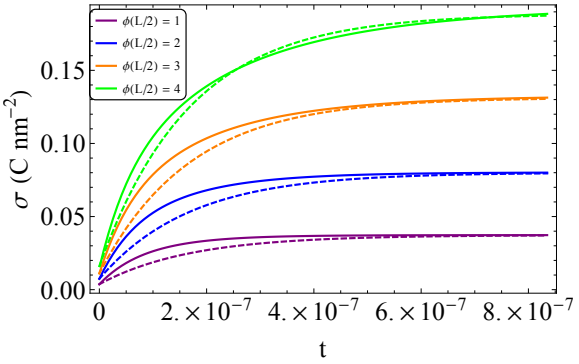

Figure 8: Surface charge development σ(+L/2)= $-\sigma$(-L/2) in time for different surface potentials. The solid line is calculated with Eq. (3), while the dashed line is calculated with $\sigma(t) = \sigma_{max} + (\sigma(0) - \sigma_{max})e^{-t/(RC)}$, where σ_{max} is the equilibrium value of σ.

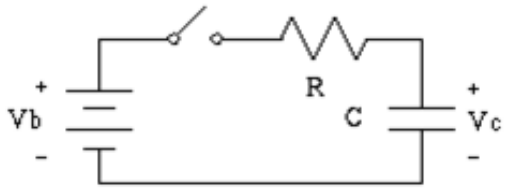

Figure 9: An RC-circuit

The development of the surface charge in time shows the same behavior as the density profiles for the half engine. For a larger surface potential, the system needs a longer time to reach equilibrium. Furthermore we can compare the surface potential of this model with the potential of an RC circuit. Our model with the two electrodes can be seen as a capacitor coupled with a resistor to a battery as is resembled in Fig. 9. The potential $V(t)$ of an RC circuit can be calculated by solving the differential equation $\frac{dV}{dt}C + V/R = 0$, which implies $V(t) = V(0)e^{-t/(RC)}$. When we use $R = \frac{L}{\sigma A}$ in which L is the length, A the area and σ the conductivity of the model, we can use Ohm's law for the current density $\overrightarrow{J} = \sigma\overrightarrow{E} = e\rho\overrightarrow{v}$, with v the speed of the ions, to determine the resistance of the model. If we combine Ohm's law with the electrostatic force $\overrightarrow{F} = e\overrightarrow{E} = 6\pi\eta a\overrightarrow{v} = \frac{\overrightarrow{v}}{\beta D}$, we get $\overrightarrow{J}/\overrightarrow{E} = e^2\rho\beta D = \sigma$. Recalling that $\kappa^2 = 4\pi\lambda_B\rho$ and $\lambda_B = \beta e^2/(4\pi\epsilon_0\epsilon)$ yields $e^2\rho_s\beta = \epsilon_0\epsilon\kappa^2$, and thus $\epsilon_0\epsilon\kappa^2 D = \sigma$. We can now derive an expression for $R = \frac{L}{A\epsilon_0\epsilon\kappa^2 D}$. If we furthermore use the formula for that describe C for ideal capacitors $C/A = Q/(VA) = \epsilon_0\epsilon\kappa/A$ and multiplying the last expression with R returns $RC = L/(\kappa D)$. The value of $RC \approx 1.7$ ns in this model. We can see in Fig. 8 that the expression $\sigma(t) = \sigma_{max} + (\sigma(0) - \sigma_{max})e^{-t/(RC)}$, where σ_{max} is the maximum value for σ in equilibrium, has a lot in common with the surface charge density or this model. The figures are not completely the same due to some assumptions in calculating RC that are not entirely true for this specific situation. For instance, the resistance R and capacitance C are not constant in our model due to fluctuation ionic density profiles, which make the capacitor non-ideal and the electrostatic force not constant in this system. On the other side, the surface charge density is quite well described by this formula and can be used to qualitatively describe the behavior of the surface charge in time.

The 61 nm model of Ref. [6] has been elaborated and we have verified the results. We extended the work from Ref. [6] by describing the the equilibrium time more in detail for different surface potentials. The system needs more time to reach equilibrium when the surface charge is high. Moreover, it is described how the surface charge density evolves in time and how this can be compared with a simple RC circuit. Now we return to our blue engine where the ions diffuse into similar charged porous electrodes. The typical width of the pores is only 2 nm, which results in different physics than the model described above. Similar charged electrodes will repel coions to the center of the model, while attracting counterions to both electrodes.

Furthermore, the Debye length is now comparable with the length of the model and we will see that this has a different effect on the diffusion of the ions. Besides the ions will need less time to diffuse from one side to the other side, thus the system will be in equilibrium much faster than the model from Ref. [6]. In the following section, a model is proposed to describe the blue engine porous electrodes.

5.2 Blue engine size electrolytic cells

Using the same model as Ref. [4], we rescale our previous model to $L = 2$ nm and the volume of the ions $v = a^3$ where $a = 0.55$ nm. The ion radius becomes $(3/(4\pi))^{\frac{1}{3}} a = 0.34$ nm which results in the diffusivity $D = 6.38 * 10^8$ m^2/s. The ionic bulk concentration is 0.1 M, which corresponds with a Debye length of $\kappa^{-1} = 1$ nm. The dimensionless quantities remain $z^* = \kappa z$, $t^* = t/\tau$ and $\phi(t, z) = \frac{e\psi(t,z)}{k_B T}$. The typical τ of for this bulk density becomes $\tau = 1.43$ ns. Two cases are described: (1) oppositely charged electrodes and (2) similar charges on the electrodes (which is the case in a blue engine). In both cases we are interested in the time it takes for the system to relax. We aim to analyze this for both a rapid charging and a more slow linear charging of the electrodes.

5.2.1 Two oppositely charged electrodes

The two electrodes are being charged with opposite charges $\phi(\pm L/2) = \pm 2$. At t=0, an initial potential $\phi(\pm L/2) = \pm 2$ is set on the electrodes, and the following potential and diffusion profiles arise (see Fig. 11).
When comparing the figures of the two models in Fig. 4 and Fig. 11 three major changes are notable. Firstly

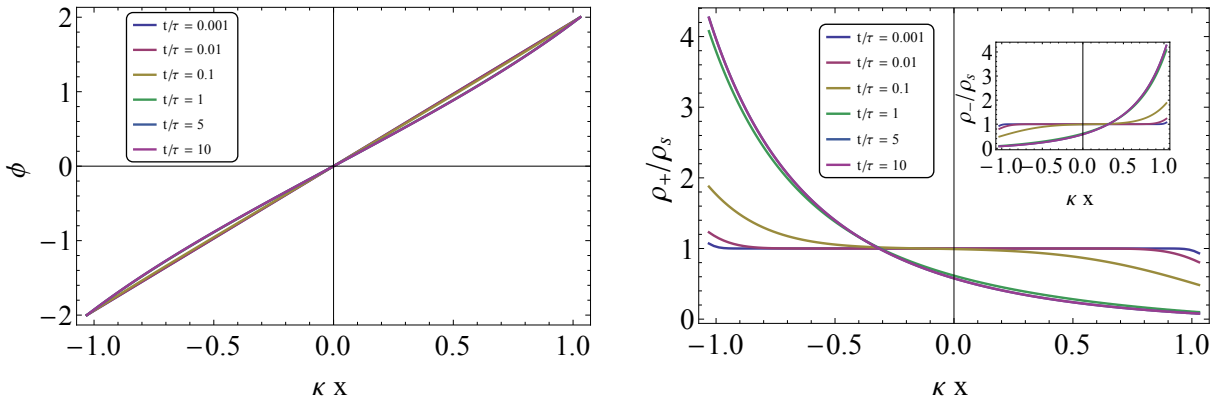

Figure 10: Potential and density profile 2 nm system with opposite surface charges set at t=0 with $\phi(\pm L/2) = \pm 2$. The potential and density profiles shift in time from $t = 0.001\tau$ (blue) to $t = 0.01\tau$ (purple), $t = 0.1\tau$ (yellow), $t = 1\tau$ (green), $t = 5\tau$ (light blue) and $t = 10\tau$ (purple).

the time to reach equilibrium is more than 10 times shorter in the 2 nm model. The 2 nm model responds much quicker because the ions do not need to diffuse a couple of Debye lengths to reach their final position. Secondly the potential profile in the 2 nm model does not differ a lot from the initial potential profile at $t = 0$. The electrodes are only 2 Debye lengths apart, and therefore the charges on the electrode cannot be screened as much as in the 61 nm model. Thirdly, the density profiles in the 2 nm model do not flatten out in the middle of the model. This is again because the electrodes are 2 Debye lengths apart and have a large influence on the whole system, whereas in the 61 nm model the major influence is limited to a couple of Debye lengths. If we again increase the potential to $\phi(\pm L/2) = \pm 4$, we get the following potential and density profiles Fig. 11. The potential en density profiles for $\phi(\pm L/2) = \pm 4$ differ not much from $\phi(\pm L/2) = \pm 2$. The system hardly responds in the potential profile, while the cations and anions very quickly attracted to the electrodes. It is remarkable that in this model, a higher surface potential results in a shorter amount of time to reach equilibrium. The system is so small that a higher surface potential results in a very high gradient of the surface potential (recall $\frac{\partial\phi(\pm L/2, t=0)}{\partial z} = \frac{\Delta\phi(t=0)}{L}$) and thus the flux $J_\pm$ is very high this system (approximately ten times higher than in the 61 nm model) in. The ions are much quicker attracted and repelled from the electrodes when the surface potential increases than in the 61 nm model. Unfortunately it is beyond the scope

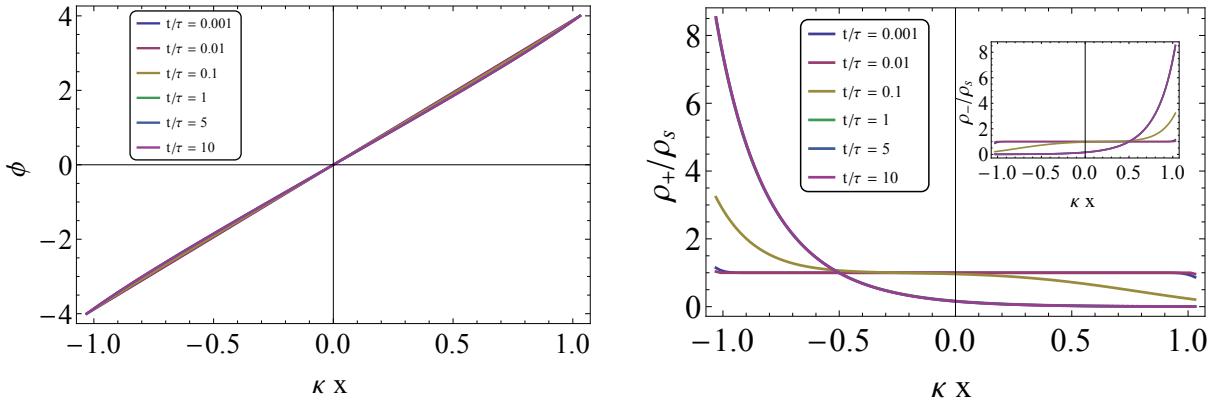

Figure 11: Potential and density profile 2 nm system with opposite surface charges set at t=0 with $\phi(\pm L/2) = \pm 4$. The potential and density profiles shift in time from $t = 0.001\tau$ (blue) to $t = 0.01\tau$ (purple), $t = 0.1\tau$ (yellow), $t = 1\tau$ (green), $t = 5\tau$ (light blue) and $t = 10\tau$ (purple).

of this project to research this relation between equilibrium time and the distance between the electrodes L more in depth.

One of the main goals of this research is to investigate how an electrolytic cell responds to a slow increase of the potential. Therefore we research how a linear increase of the surface charge influences the system. We do this for five different linear increases of the potential, which are displayed in Fig. 12. The time t^{**} is used as the time at which the surface potential has reached its maximum value in such a way that $\phi(\pm L/2, t = t^{**}) = \pm 2$. To investigate the equilibrium time for this slow increase of the surface potential, we

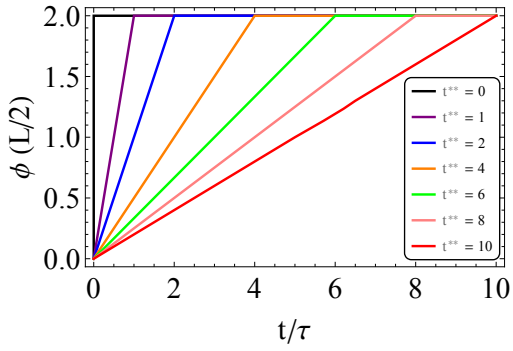

Figure 12: Linearly increasing the surface charge on the electrodes. The surface potential for $\phi(\pm L/2)_{max} = \pm 2$ is reached for different linear charging methods at time t^{**}. For example, if $t^{**} = 1$, the surface potential has reached the maximum value $\phi(\pm L/2, t = t^{**}) = \pm 2$ after one diffusion time $t/\tau = 1$.

can again consider half of the model and add up the density profiles or calculate the surface charge on the electrodes. This is shown in the Fig. 13 and Fig. 14. Obviously the time to reach equilibrium takes longer when the electrodes are slowly being charged within a long amount of time. The ions are constantly triggered by a small increase of the potential and are constantly moving a small bit towards equilibrium. If the electrodes are very slowly charged up, e.g. $t^{**} = 10$, the system reaches equilibrium at every timestep t/τ for that specific surface charge. This can be seen in Fig. 13 and Fig. 14 where the density profiles and surface charges are linearly correlated with t/τ. This is analyzed further by introducing the equilibrium time t_{eq} which states the time when the system has reached equilibrium. If we plot the equilibrium time versus t/τ, we can relate the time to reach equilibrium for charging the electrodes within a certain amount of time. Fig. 15 presents this correlation.

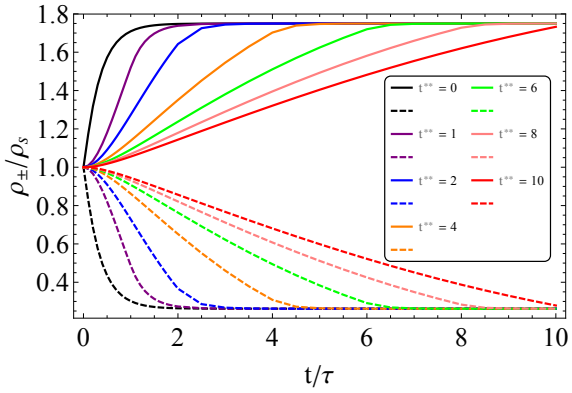

Figure 13: Integration of the ion densities for $-L/2 < z \leq 0$. The solid lines represent the addition of the densities of the cations and the dashed lines represent this addition for the anions. The time to reach equilibrium increases when the t^{**} on the electrodes increases.

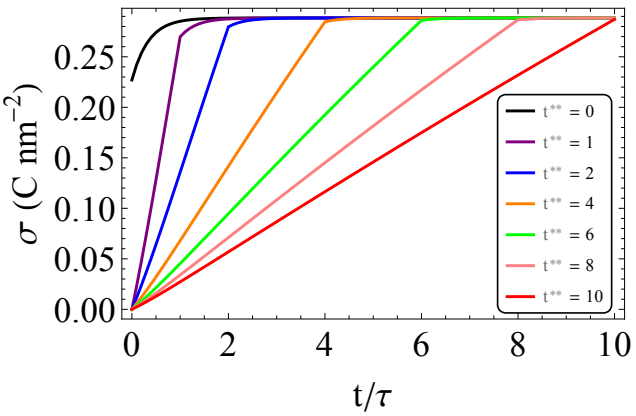

Figure 14: Surface charge development σ(+L/2)= $-\sigma$(-L/2) in time for different linear charging procedures of the electrode. The solid line is calculated with Eq. (3)

In Fig. 15, we observe a linear correlation between t_{eq}/τ and t^{**}. As stated before, the difference

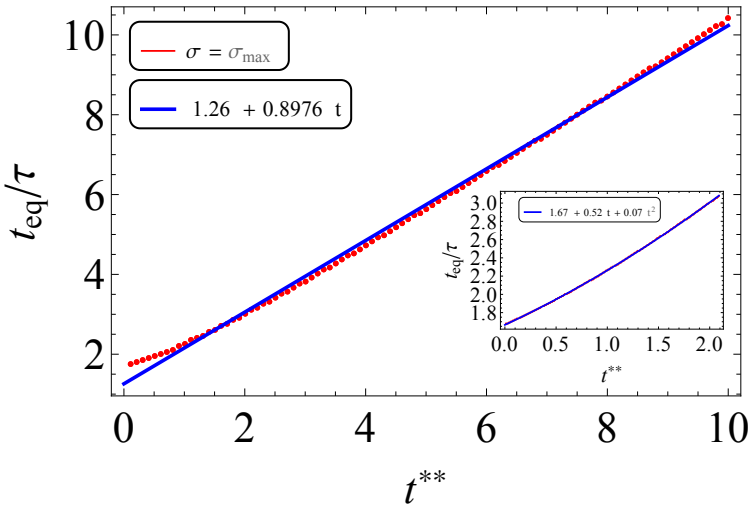

Figure 15: The time to reach equilibrium t_{eq} as a function of t^{**}. The inner figure zooms in on the most interesting part where $t_{eq}/\tau < 1 + t^{**}$ and the beavior is not linear.

between t_{eq}/τ and t^{**} decreases when t^{**} is large in such a way that the ions have enough time to reach equilibrium at every timestep. However, when we zoom in on $t^{**} < 2$, the inner figure in Fig. 15, the relation between t_{eq}/τ and t^{**} becomes quadratic and can be described with the formula stated in the inner figure. This is mainly due to the initial time that the model needs to reach equilibrium, which is about 1.67 t/τ. After $t^{**} \gtrsim 4$, this relationships between the equilibrium time and the charging time becomes linear and stays linear.

In summary, when comparing the 61 nm model from Ref. [6] and the 2 nm model, we noted that the potential and density profiles are very different and that the electrodes have a larger influence on the whole system in the 2 nm model than in the 61 nm model where the influence is mainly limited to a couple Debye lengths. We also noted that in the 2 nm model the ions responds much quicker than in the 61 nm model.

Moreover, if the surface potential is increased, the time to reach equilibrium is decreased in the 2 nm model, but increased in the 61 nm model. Probably this is influenced by the amount of the Debye lengths between the electrodes. Finally, a linear increase of the surface potential in time is researched and it is concluded that the relation between the time for the system to reach equilibrium is linear correlated with the time to charge up the electrodes. When looking at quick potential increases, this relationship between the equilibrium time and the time to charge the electrodes becomes quadratic. But what happens when the electrodes have a similar charge on the plates $\phi(-L/2,t) = \phi(+L/2,t)$. This problem is described in the following section.

5.2.2 Two similarly charged electrodes

In this case, the previous 2 nm model is used with one big difference, the surface potential on the electrodes is equal $\phi(-L/2,t) = \phi(+L/2,t)$. If we take $\phi(-L/2,t)$ positive, it is possible to generate the same results for a negetatively charged electrode. The Nernst-Planck equation Eq. (12) can be used again with the same procedure to calculate the density profiles. However, one problem arises. When calculating the first initial gradient of the potential $\frac{\partial\phi(z,t=0)}{\partial z} = \frac{\phi(L/2,0)-\phi(-L/2,0)}{L} = 0$ and the flux $J_{\pm} = 0$ as well. This implies that nothing will happen in the symmetric system unless there is a perturbation which causes an asymmetry and triggers the system to respond. If we zoom out from our porous electrodes and look at a real blue engine and the electrodes of a couple microns apart, the positively charged electrode and negatively charged electrode are mainly in contact with counterions. The counterions flow into the pores of the electrodes and cause an asymmetry in the pores due to this flow and the excess number of counterions versus the low number of coions.

In order to use our model and describe how the system evolves in time, we impose a symmetry breaking for the initial state. The proposed symmetry breaking assumes that the potential in the center of the model is equal to zero at t =0. This implies a gradient in the potential, and the system start evolving in time by colliding the cations in the center between the electrodes and the anions moving out towards the electrodes. Note that the following figures Fig. 16, Fig. 17 and Fig. 18 are made with this symmetry breaking and are more a qualitative description of the reality. In Fig. 16 the development of the potential is shown.

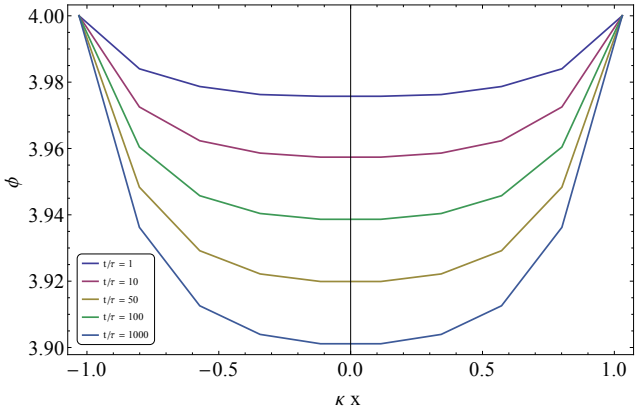

Figure 16: Development of a potential profile in time for $\phi(-L/2) = \phi(L/2) = 4$. The timescale are $t/\tau = 1$ (blue), t/τ =10 (purple), t/τ =50 (green), $t/\tau = 100$ (yellow) and $t/\tau = 1000$ (blue)

At the start of this development, when $t/\tau \approx 0.1$, the potential profiles respond very quickly to the gap in the potential and rearrange into an almost linear potential profile. Thereafter, the model evolves into time by decreasing the potential in the middle. Anions are attracted to the electrodes and anions are repelled to the center of the system, which can also be seen in Fig. 17 and Fig. 18. The ions keep screening the potential up to $t/\tau = 1000$, which is quite a long time for this model (about 100 times the time for opposite charges). Another strange outcome is that particle number is not conserved in this situation. The total number of cations decreases in time, while the total number of anions increases. Apparently, when stating the potential to be zero at the center of the model imposes ions to flow into and out of the system. Although this last simulation is forced by a perturbation and does not predict quantitatively what happens when two similarly charged electrodes are used in the model, it qualitatively describes the motion of the cations and anions well

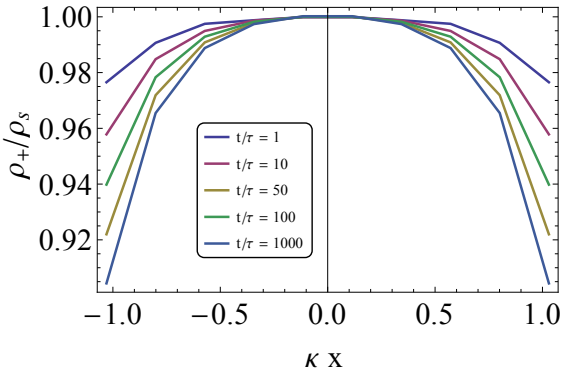

Figure 17: Development of the cation density ρ_+ profile in time for $\phi(-L/2) = \phi(L/2) = 4$. The timescale are $t/\tau = 1$ (blue), t/τ =10 (purple), t/τ =50 (green), $t/\tau = 100$ (yellow) and $t/\tau = 1000$ (blue)

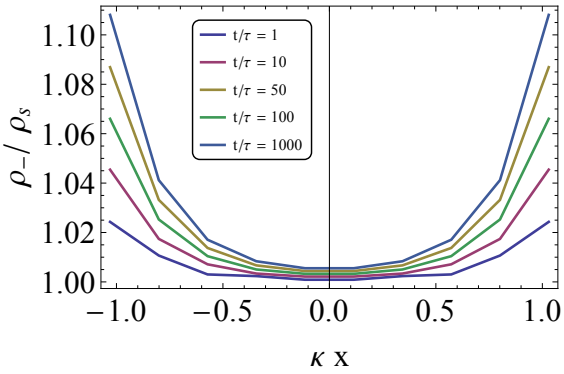

Figure 18: Development of the anion ρ_- density potential profile in time for $\phi(-L/2) = \phi(L/2) = 4$. The timescale are $t/\tau = 1$ (blue), t/τ =10 (purple), t/τ =50 (green), $t/\tau = 100$ (yellow) and $t/\tau = 1000$ (blue)

and also predicts the development of the potential.

6 Conclusion and discussion

A blue engine makes use of the chemical potential difference between fresh and seawater to generate energy. A simple blue engine consists two porous electrodes a couple of microns apart. When seawater flushes through the electrodes and a surface charge is put on the electrodes, the ions in the seawater will move into the pores of the electrodes which have a typical thickness of 2 nm. Thereafter fresh water is led between the electrodes and the electrodes are discharged, which causes the ions to move into the fresh water. In this way, energy is generated by using the entropy of mixing from the seawater that becomes a bit more fresh and the fresh water that becomes a bit more salty. Most models describing a blue engine only take into account the equilibrium potential and ionic density profiles. However, since the ions respond less quick than the charges on the electrodes, the time is an important factor in a blue engine. More specifically, dynamics are important when the total power output, which is energy per time, is concerned. Therefore this research investigated the dynamics of dissolved charged particles in electrolytic cells. Three models containing two electrodes at $-L/2$ and $+L/2$ and a bulk density ρ_s of ions dissolved in water are described. These models are used to investigate the time for the system to reach equilibrium and to research what happens when the surface charge on the electrodes is increased within time. The Nernst-Planck equation in combination with the Poisson-Boltzman equation with a constant diffusivity are used to calculate the potential, density profiles and flux profiles of the systems.

The first model was also used by Ref. [6] and is used to verify the results. The model consists of a 61 nm electrolytic cell, a bulk density ρ_s =10mM and a radius of the ions a =0.2 nm. The electrodes have opposite charges. The potential, density and flux profiles for $\phi(\pm L/2) = \pm 2$ and ± 4 were presented. The potential profile and the density profiles are mainly influenced near the elctrodes, up to a couple Debye lengths from the electrodes. When the surface potential is increased, the system needs more time to reach equilibrium. This can specifically be seen when adding the density profiles for half of the engine or calculating the surface charge density. Moreover, the surface charge density evolves in time somewhat like a potential in an RC circuit evolves in time. The time for the system to reach equilibrium varies between (20 - 100) * 8.4 ns for a dimensionless surface potential between 1 - 4.

The second model describes two electrodes with opposite charges that are a distance 2 nm apart. Furthermore, ρ_s= 0.1M and the particles have a size of a= 0.55. This second model reacts much quicker than the first model on the imposed surface potential and reaches equilibrium within 3 ns for the dimensionless

surface potential 2. This has to do with the short size, only 2 Debye lengths, of the system, which implies a quick reaction. The potential profile does not change much in comparison with the initial potential profile at $t = 0$, but the density profiles are very much influenced by the surface potential on the electrodes. When charging the electrodes slowly, the relation between reaching equilibrium and the time that the electrodes are fully charged is linear. When charging the electrodes more quickly, this relation becomes more quadratic.

The third model aims to describe the porous electrodes of a blue engine. The model is the same as the second model, but has similarly charged electrodes instead of oppositely charged electrodes. Unfortunately, the model is too simple to describe what really happens in the porous electrodes. Because the gradient of the potential is zero, the flux is also zero and the symmetric system remains in equilibrium. In a real blue engine, ions flow in an out the pores and impose an asymmetry in the model. In this research we perturb the system by stating that the potential is zero in the center of the electrolytic cell. The out coming potential and density profiles are quantitatively not correct, but qualitatively describe how the system should react. The potential profile is lowered in the middle of model, cations are repelled to the center and anions are attracted to the electrodes. Perhaps it is a nice idea for a next BONZ to research this particular problem more into depth and to develop a code or perturbation that will describe the behavior in a blue engine pore correctly

This research has added to the comprehension of the dynamics of ions in electrolytic cells. Unfortunately it was not possible to connect the final outcomes to the blue engine because of the symmetry problem of the third model. However, when this research is continued, it is possible to extend the third model and couple the model to an external ion bath. When ions can flow in and out of the model, the pores of the electrodes in a blue engine can be properly described and the optimal time per cycle can be calculated in combination with the work from Ref. [4]. Moreover, it will be interesting to calculate for which sizes of the electrode the time to reach equilibrium increases or decreases for a higher potential. When doing this for similarly charged electrodes, the optimal porous size can be calculated which will decrease the time per cycle and optimizes the power output per cycle.

References

[1] J. Chmiola, G. Yushun, Y.Gogotsi, C. Portet, P. Simon and P.L. Taberna, Science **313**, 1760 (2006).

[2] J.R. Millar and P. Simon, Science **321**, 651 (2008).

[3] Brogioli D., Phys. Rev. Lett., **103**, 058501 (2009).

[4] N. Boon and R. van Roij, Mol. Phys. **109**, 1229 (2011).

[5] A. A. Kornyshev, J. Phys. Chem B. **111** (20), 5545-5557 (2007).

[6] I. C. Gârlea. Dynamics of charged particles in an electrolytic cell with an oil-water interface (2010). Master thesis Institute for Theoretical Physics Utrecht University.

[7] Gouy L. G., J. Phys. (Paris), 9, **475**. (1910).

[8] Chapman D. L., Philos. Mag., 25, **475** (1913).

[9] M.M. Hatlo, R. van Roij and L. Lue, Eurphys. Lett **97**, 28010 (2012).

[10] International Association for the Properties of Water and Steam. International Towing Tank Conference (2011). Accessible via `http://ittc.sname.org/CD%202011/pdf%20Procedures%202011/7.5-02-01-03.pdf`.

[11] W. H. Press, S.A. Teukolsky, W.T. Vetterling, B.P. Flannery, Numerical Recipes 3rd Edition: The Art of Scientific Computing (2007). Cambridge University Press, New York.

7 Appendix

7.1 Tridiagonal matrix

We use a tridiagonal matrix to solve the PB-equation and make use of the code as stated in the book Numerical Recipes [11] (pp. 48-57). Using this code, a double derivative is approximated with a tridiagonal matrix working on a potential. When discretizing the system, we can write the first derivative for $\phi'(z_i)$ with step size h as $\phi'(z_i) = \frac{\phi(z_i+h)-\phi(z_i)}{h}$ or as $\phi'(z_i) = \frac{\phi(z_i+h)-\phi(z_i-h)}{h}$. The second derivative becomes a combination of these two $\phi''(z_i) = \frac{\phi(z_i+h)-2\phi(z_i)+\phi(z_i-h)}{h^2}$, which is symplified by $\phi_i'' = \frac{\phi_{i+1}-2\phi_i+\phi_{i-1}}{h^2}$ where i determines the position z_i. The PB-equation must be calculated for every ϕ_i from ϕ_0 up to ϕ_n where $n = L/h$ is the total number of positions. So the left-hand side of the PB-equation consists of a matrix containing elements $\begin{pmatrix} 1 & -2 & 1 \end{pmatrix}$ on the diagonals times the potential $\begin{pmatrix} \phi_{i-1} \\ \phi_i \\ \phi_{i+1} \end{pmatrix}$. The right-hand side of the PB equation is then equal to $-4\pi\lambda_{\mathrm{B}} q(z) = \begin{cases} \phi_{\mathrm{plate}} \text{ for } i = 0 \text{ or } i = n \\ -4\pi\lambda_{\mathrm{B}}(\rho_+(z) - \rho_-(z)) \text{ otherwise} \end{cases}$. The following equation arises

$$\begin{pmatrix} -2 & 1 & 0 & 0 & \cdots & 0 & 0 & 0 & 0 \\ 1 & -2 & 1 & 0 & \cdots & 0 & 0 & 0 & 0 \\ 0 & 1 & -2 & 1 & \cdots & 0 & 0 & 0 & 0 \\ \vdots & \vdots & \ddots & \ddots & \ddots & \vdots & \vdots & \vdots & \vdots \\ \vdots & \vdots & \vdots & \ddots & \ddots & \ddots & \vdots & \vdots & \vdots \\ \vdots & \vdots & \vdots & \vdots & \ddots & \ddots & \ddots & \vdots & \vdots \\ 0 & 0 & 0 & 0 & \cdots & 1 & -2 & 1 & 0 \\ 0 & 0 & 0 & 0 & \cdots & 0 & 1 & -2 & 1 \\ 0 & 0 & 0 & 0 & \cdots & 0 & 0 & 1 & -2 \end{pmatrix} \times \begin{pmatrix} \phi_0 \\ \phi_1 \\ \phi_2 \\ \vdots \\ \vdots \\ \vdots \\ \phi_{n-2} \\ \phi_{n-1} \\ \phi_n \end{pmatrix} = -4\pi\lambda_{\mathrm{B}} \begin{pmatrix} \frac{\phi(-L/2)}{-4\pi\lambda_{\mathrm{B}}} \\ \rho_{1,+} - \rho_{1,-} \\ \rho_{2,+} - \rho_{2,-} \\ \vdots \\ \vdots \\ \vdots \\ \rho_{n-2,+} - \rho_{n-2,-} \\ \rho_{n-1,+} - \rho_{n-1,-} \\ \frac{\phi(L/2)}{-4\pi\lambda_{\mathrm{B}}} \end{pmatrix},$$

in which $\phi(-L/2)$ and $\phi(L/2)$ stand for the potential on the left and right plates respectively. This equation can be solved by setting some initial values for the potential on the plates, calculate the density profiles with this potential and inverting the tridiagonal matrix. The used code for inverting a tridiagonal matrix is presented in Numerical Recipes [11]